

# Superconducting Detectors for Super Light Dark Matter

Yonit Hochberg,<sup>1</sup> Yue Zhao,<sup>2</sup> and Kathryn M. Zurek<sup>1</sup>

<sup>1</sup>*Theoretical Physics Group, Lawrence Berkeley National Laboratory, Berkeley, CA 94720  
Berkeley Center for Theoretical Physics, University of California, Berkeley, CA 94720*

<sup>2</sup>*Stanford Institute for Theoretical Physics, Department of Physics,  
Stanford University, Stanford, CA 94305, U.S.A.*

We propose and study a new class of superconducting detectors which are sensitive to  $\mathcal{O}(\text{meV})$  electron recoils from dark matter-electron scattering. Such devices could detect dark matter as light as the warm dark matter limit,  $m_X \gtrsim 1 \text{ keV}$ . We compute the rate of dark matter scattering off free electrons in a (superconducting) metal, including the relevant Pauli blocking factors. We demonstrate that classes of dark matter consistent with all astrophysical and terrestrial constraints could be detected by such detectors with a moderate size exposure.

**Introduction.** The search for the identity of dark matter (DM) is in an exciting and rapidly developing era. Theories of weakly interacting massive particles (WIMPs) for DM, being predictive and testable, have been the primary focus of both theory and experiment for the last thirty years. Strong constraints from direct detection experiments, such as Xenon100 [1], LUX [2] and SuperCDMS [3], along with the absence of new physics signals from the LHC, have, however, been painting such models as increasingly constrained and tuned. Further, because the energy threshold of direct detection experiments searching for WIMPs is typically 1-10 keV, these experiments lose sensitivity to DM particles with mass below 10 GeV. At the same time, DM candidates with low masses are theoretically well-motivated: asymmetric dark matter [4, 5] and strongly interacting massive particles [6] are examples in which the natural mass scale of the DM sits beneath the  $\sim 10 \text{ GeV}$  scale.

A new frontier for massive DM thus opens for  $1 \text{ keV} \lesssim m_X \lesssim 10 \text{ GeV}$ , with the lower bound set approximately by warm dark matter constraints, *e.g.* from phase space packing [7, 8] or the Lyman- $\alpha$  forest [9]. For elastic scattering processes, the deposited energy is  $E_D \simeq q^2/(2m_{e,N})$ , where  $q \sim \mu_r v_X$  is the momentum transfer with  $v_X \sim 10^{-3}$  the incoming DM velocity,  $\mu_r$  the reduced mass of the system and  $m_{e,N}$  is the mass of the target electron or nucleus  $N$ . Thus for 100 MeV DM, an eV of energy is deposited for scattering off a nucleus. Inelastic processes, such as electron ionization or excitation above a band gap, may occur when the DM kinetic energy exceeds the binding energy. Utilizing a semi-conducting crystal such as germanium, with a band gap of 0.7 eV, implies potential sensitivity to DM as light as  $\mathcal{O}(\text{MeV})$  [10, 11]. SuperCDMS is already working to lower its threshold to 300 eV [3], constraining 1 GeV mass DM.

To go well below this, as low as the warm DM limit at  $\mathcal{O}(\text{keV})$ , requires a different kind of technology; in this case one must be able to access electron recoil energies as low as  $\mathcal{O}(\text{meV})$ . The purpose of this letter is to investigate a proof of principle experiment to search for DM

down to the warm DM limit. Devices utilizing superconductors, we will show, are ideal for this purpose, as they can be sensitive to extremely small energy depositions. In fact, in cold metals, the limit on the sensitivity of the experiment to low energy DM recoils is set by the ability to control the noise rather than by an inherent energy gap in the detector.

The targets we discuss are metals, with the DM interacting with free electrons in the Fermi sea. The DM scattering rate is limited by Pauli blocking for electrons locked deep in the sea, yielding a suppression factor of order the energy transfer over the Fermi energy; the suppression is, *e.g.*, of order  $\sim 10^{-4}$  for a DM-electron scattering with meV energy deposition in a typical metal such as gold or aluminum. As we will show, DM models satisfying all astrophysical and terrestrial constraints are detectable despite the Pauli blocking effect, extending the conceptual reach of the detection method down to DM masses of  $\mathcal{O}(\text{keV})$ .

**Detection with Superconductors.** The challenge in designing a detector to observe DM depositing very little energy is to achieve a large target mass, while keeping noise low. Detection of small energy depositions is by now well-established; superconductors, with a meV superconducting-gap, have sensitivity to energies at this scale. Transition edge sensors (TES) and Microwave Kinetic Inductance Devices (MKIDs) have been utilized to detect microwaves and x-rays with sub-meV to keV energies in astrophysical applications. For example, TESs with sensitivity to energy depositions not very far from our range of interest already exist: Refs. [12–14] have demonstrated noise equivalent power in the range  $\sim 10^{-19} - 10^{-20} \text{ W}/\sqrt{\text{Hz}}$ . This translates to a sensitivity of  $\sim 50 - 300 \text{ meV}$  of energy over a read-out time of  $\sim 10 \text{ ms}$ . While not quite at the level of sensitivity needed, further improvement could be made by lowering both the heat bath temperature (from, for instance, 100 mK to 10 mK) and decreasing the heat capacitance of the TES by reducing the volume.

The TES and MKID, however, have very low masses — an MKID is typically a nano-gram in weight, while

TESs are approximately 50 microns on a side and a fraction of a micron thick. As a result, they do not make good detectors themselves. Their masses cannot simply be increased since this would decrease their sensitivity to small deposits of energy. An alternative is then to use the TES or the MKID merely as heat sensors which register small deposits of energy from a much larger target mass, an ‘absorber.’

As a DM particle hits a free electron in the Fermi sea of the absorber, if the absorber itself is a superconductor, the recoiling electron will deposit an  $\mathcal{O}(1)$  fraction of its energy into breaking Cooper pairs, creating quasiparticles in the superconductor. These quasiparticles random walk in the superconductor until they either (I) recombine and create an athermal phonon or (II) are absorbed. In the former case, the athermal phonon may break Cooper pairs in the MKID, leading to an observable change in the kinetic inductance. In the latter case, the quasiparticles may reach a collection fin on the surface of the absorber. The quasiparticles thermalize as soon they reach the collection fins, which are connected to the TES which registers the heat. The quasiparticle lifetimes are sufficiently long (well in excess of  $\mu\text{s}$ ) and their velocities sufficiently high (up to the Fermi velocity,  $\sim 10^{-2}c$ ) that even if the collection fin area on the absorber is small, the quasiparticles ricochet sufficiently many times that they are very efficiently channeled from the absorber into the collection fins and on to the TES. In either case, the MKID or the TES is acting as a calorimeter for the energy deposited in the absorber. The underlying design principle sketched here is of concentration: one seeks to store the deposited energy non-thermally, whether through quasiparticles or athermal phonons, and then concentrate them through a collection mechanism onto the MKID or TES. This process must happen fairly rapidly, on the timescale of a millisecond.

Our purpose here is not to design a detector in detail, rather simply to outline how, on the timescale of a decade, sensitivity to extremely light DM utilizing superconducting technology may be feasible. The remainder of this letter focuses on the reach of such an experiment into the parameter space of light dark matter.

**Rates and Backgrounds.** Detection via TESs (or MKIDs) operates by DM scattering off of free electrons in a metal. In a superconductor, the free electrons are bound into Cooper pairs, which typically have  $\sim \text{meV}$  (or less) binding energy. Once the energy in the scattering exceeds this superconducting gap, however, the scattering rate is computed by the interaction with free electrons. These electrons are described by a Fermi-Dirac distribution at low temperature. The typical Fermi energy  $E_F$  of these electrons is  $p_F^2/(2m_e) \sim 10 - 100 \text{ eV}$ , with  $p_F \sim 10 \text{ keV}$  in a typical metal such as aluminum or gold.  $E_F$  sets how deeply buried a target electron is in the Fermi sea, and how much energy must be transferred in the scattering in order to pull an electron out of the

sea. As a result, with kinetic energy of the incoming DM approximately  $m_X v_X^2 \sim \text{meV} - \text{keV}$  for keV to GeV DM, Pauli blocking is important for the DM scattering rate. We follow the discussion in [15] to compute the rate correctly, factoring in the Pauli blocking effect. We denote the 4-momentum of DM initial and final states by  $P_1$  and  $P_3$ , the initial and final states of the electron by  $P_2$  and  $P_4$ , and the momentum transfer  $q = (E_D, \mathbf{q})$ . The scattering rate can be estimated via

$$\langle n_e \sigma v_{\text{rel}} \rangle = \int \frac{d^3 p_3}{(2\pi)^3} \frac{\langle |\mathcal{M}|^2 \rangle}{16 E_1 E_2 E_3 E_4} S(E_D, |\mathbf{q}|), \quad (1)$$

$$S(E_D, |\mathbf{q}|) = 2 \int \frac{d^3 p_2}{(2\pi)^3} \frac{d^3 p_4}{(2\pi)^3} (2\pi)^4 \delta^4(P_1 + P_2 - P_3 - P_4) \times f_2(E_2)(1 - f_4(E_4)),$$

where  $E_D$  is the deposited energy,  $\langle |\mathcal{M}|^2 \rangle$  is the squared scattering matrix element summed and averaged over spin, and  $f_i(E_i) = [1 + \exp(\frac{E_i - \mu_i}{T})]^{-1}$  is the Fermi-Dirac distribution of the electrons at temperature  $T$ .  $S(E_D, |\mathbf{q}|)$  characterizes the Pauli blocking effects, and in the limit of  $T \rightarrow 0$ ,  $S(E_D, |\mathbf{q}|)$  reduces to a simple Heaviside theta function, with amplitude  $m_e^2 E_D / (\pi |\mathbf{q}|)$ . We perform the integral numerically in order to capture the entire kinematic range properly. The total rate (per unit mass per unit time) is then

$$E_D \frac{dR_{\text{DM}}}{dE_D} = \int dv_X f_{\text{MB}}(v_X) E_D \frac{d\langle n_e \sigma v_{\text{rel}} \rangle}{dE_D} \frac{1}{\rho} \frac{\rho_X}{m_X}. \quad (2)$$

Here  $\rho$  is the mass density of the detector material, and  $\rho_X = 0.3 \text{ GeV/cm}^3$  the DM mass density. We take the velocity distribution of the DM  $f_{\text{MB}}(v_X)$  to be a modified Maxwell Boltzmann with rms velocity  $v_0 = 220 \text{ km/sec}$ , and cut-off at the escape velocity  $v_{\text{esc}} = 500 \text{ km/sec}$ . Since the typical Fermi velocity of a metal is  $v_F = \mathcal{O}(10^3) \text{ km/sec} \gg v_{\text{esc}}$ ,  $v_{\text{rel}} \simeq v_F$ . The Pauli blocking effect provides a suppression factor of order  $E_D/E_F$ , which we confirm numerically. An irreducible background is expected to come from neutrinos, which, due to the low energy deposition in the detector, will be dominated by  $pp$  neutrinos [16, 17]. We find that the solar neutrino background is many orders of magnitude below the signals we consider, and is hence omitted from further discussion.

In what follows we assume that the DM  $X$  interacts with electrons via exchange of a mediator  $\phi$ . The generalization of light DM models will be addressed in future work [18]; we seek only to demonstrate proof of principle here. The scattering cross section between, *e.g.*, Dirac DM and free electrons is given by  $\sigma_{\text{scatter}} = 16\pi \alpha_e \alpha_X \mu_{eX}^2 / (m_\phi^2 + q^2)^2$ , where  $\alpha_i \equiv g_i^2/(4\pi)$ ,  $g_i$  is the coupling of  $\phi$  to  $i$  with  $i = e, X$ ,  $\mu_{eX}$  the reduced mass of the electron-DM system, and  $q$  the momentum transfer in the process. This cross-section is related to the matrix element in Eq. (1) via  $\sigma_{\text{scatter}} = \frac{\langle |\mathcal{M}|^2 \rangle}{16\pi E_1 E_2 E_3 E_4} \mu_{eX}^2$ .

We define two related reference cross sections  $\tilde{\sigma}_{\text{DD}}$ , corresponding to the light and heavy mediator regimes:

$$\begin{aligned}\tilde{\sigma}_{\text{DD}}^{\text{light}} &= \frac{16\pi\alpha_e\alpha_X}{q_{\text{ref}}^4}\mu_{eX}^2, \quad q_{\text{ref}} \equiv \mu_{eX}v_X, \\ \tilde{\sigma}_{\text{DD}}^{\text{heavy}} &= \frac{16\pi\alpha_e\alpha_X}{m_\phi^4}\mu_{eX}^2,\end{aligned}\quad (3)$$

where  $v_X = 10^{-3}$ . The transition between these regimes is set by how large the mediator mass is in comparison to the momentum transfer. The reference momentum transfer  $q_{\text{ref}}$  above is chosen for convenience as a typical momentum exchange. Note however that for a light mediator, the direct detection cross section is determined by the minimal momentum transfer in the process, which is controlled by the energy threshold of the detector.

To establish a notion of the expected number of events, in Fig. 1 we present the differential rate per kg-year as a function of deposited energy for several benchmark points described in the next section. When the mediator is effectively massless, namely lighter than the momentum transfer in the scattering, the rate is peaked at energies near the detector threshold. In contrast, for massive mediators, the rate is peaked at higher recoil energies. The reason for the latter behavior is that as the recoil energy increases, more electrons can be pulled from deeper in the Fermi sea, resulting in an increased rate. The mass of the mediator determines the scattering distribution in phase space, but does not control the size of the available phase space. A cutoff in the differential rate is evident for both light and heavy mediators, and depends on the DM mass. For heavier DM (dashed curves), the maximum energy deposition is determined by  $E_D^{\text{max}} = \frac{1}{2}m_e((v_F + 2v_{\text{esc}})^2 - v_F^2)$ . When the DM is lighter (solid curves), the cutoff is determined by the kinetic energy of the DM, namely by  $\mu_{eX}v_{\text{esc}}^2/2$ .

**Results.** In Fig. 2 we show the 95% expected sensitivity reach after one kg-year exposure, corresponding to the cross section required to obtain 3.6 signal events [19]. The left (right) panel corresponds to the light (heavy) mediator regime, where we plot  $\tilde{\sigma}_{\text{DD}}^{\text{light}}$  ( $\tilde{\sigma}_{\text{DD}}^{\text{heavy}}$ ) as a function of  $m_X$ . The black solid [dashed] curve in both panels corresponds to a sensitivity to measured energies between 1 meV–1 eV [10 meV–10 eV]. For light mediators, the scattering rate is sensitive to the lowest energy depositions, resulting in a large improvement in reach when the detector threshold is decreased. For massive mediators, the differential rate peaks towards larger energies, though with a lower threshold there is more sensitivity to lighter particles.

The next important question is what range of cross-sections in Eq. (3) are consistent with astrophysical and terrestrial constraints on the couplings  $\alpha_e$  and  $\alpha_X$  of  $\phi$  to electrons and DM. We divide our discussion into light mediator and heavy mediator regimes. We begin with a light mediator, focusing on a kinetically mixed hidden photon

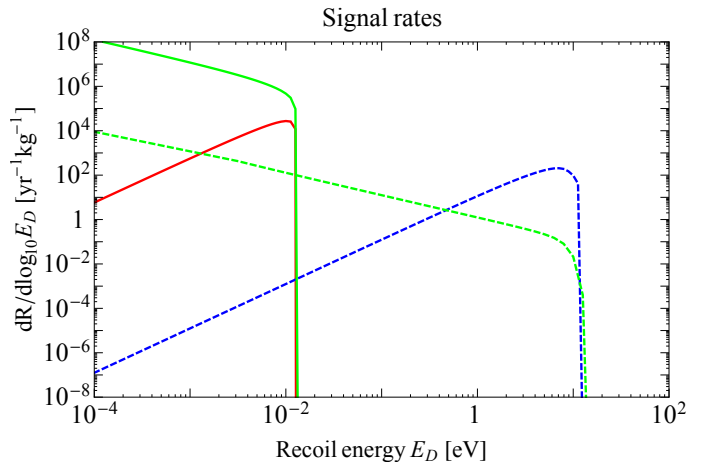


FIG. 1: Signal rates per kg-year, for several benchmark points of  $(m_\phi, m_X, \alpha_X, g_e) = (10 \mu\text{eV}, 10 \text{ keV}, 5 \times 10^{-14}, 3 \times 10^{-9})$  [solid green],  $(10 \mu\text{eV}, 100 \text{ MeV}, 5 \times 10^{-8}, 3 \times 10^{-12})$  [dashed green],  $(1 \text{ MeV}, 10 \text{ keV}, 0.1, 3 \times 10^{-6})$  [solid red], and  $(100 \text{ MeV}, 100 \text{ MeV}, 0.1, 3 \times 10^{-5})$  [dashed blue]. We use the Fermi energy of aluminum,  $E_F = 11.7 \text{ eV}$ . The green [red and blue] curves correspond to a particular DM mass along the same-colored curve in the left [right] panel of Fig. 2.

$\phi$  that obtains its mass via a dark Higgs mechanism, with  $\epsilon$  the kinetic mixing parameter. Diagonalizing the kinetic terms and moving to the mass basis, the hidden photon couples to the electromagnetic current of the SM with strength  $g_e = e\epsilon$ . The strongest constraint on this coupling, when  $m_\phi \lesssim 1 \text{ keV}$ , comes from cooling in horizontal branch stars and the sun [20, 21]. Depending on the size of  $\alpha_X$ , either dark Higgsstrahlung processes bound  $\sim \alpha_e\alpha_X$ , assuming the dark Higgs and DM have similar charges to  $\phi$ , or direct emission of  $\phi$  bounds  $\alpha_e$  itself. A bound on  $\alpha_X$  is derived from DM self-interactions—the bullet-cluster [22–24] along with recent simulations which reanalyze the constraints from halo shapes [25, 26], limit the DM self-interacting cross section (at velocities  $\gtrsim 300 \text{ km/sec}$ ) to be  $\sigma_T/m_X \lesssim 1 \text{ cm}^2/\text{g}$ , where we use the full expressions for (the classical regime of)  $\sigma_T$  found *e.g.* in Ref. [27]. The self-scattering constraint on  $\sigma_T$  then places an upper bound on  $\alpha_X$  for a given  $m_\phi$  and  $m_X$ . Lastly, we check that the DM remains out of kinetic equilibrium with the baryons up through the time of recombination [28].

In the left panel of Fig. 2 we plot the largest allowed direct detection cross section  $\tilde{\sigma}_{\text{DD}}^{\text{light}}$  [Eq. (3)] consistent with all constraints, for a variety of light mediator masses  $m_\phi \lesssim \text{eV}$ , shown in solid colored curves. As is evident, large direct detection cross sections can be obtained despite the severe bounds on the couplings. This is due to the large enhancement factor in Eq. (3), that scales like four powers of the inverse of the momentum transfer in the detection process when the mediator is light. The

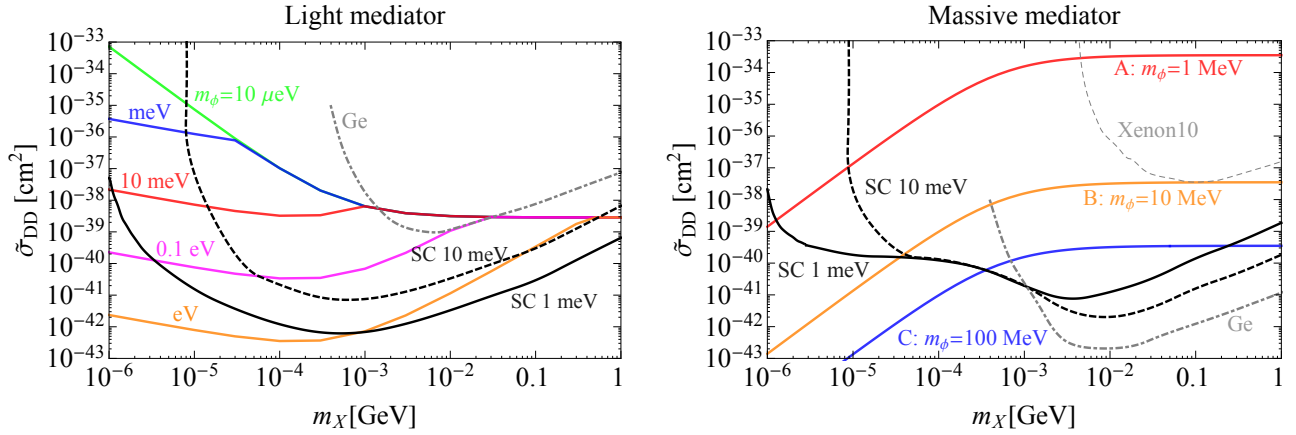


FIG. 2: **Left:** Upper bounds on direct detection cross section for light dark matter scattering off electrons, for very light mediators. Constraints arise from stellar cooling processes [20, 21], bullet-cluster and halo shapes [22–26], as well as kinetic decoupling during recombination epoch [28]. **Right:** Direct detection cross section between light dark matter and electrons, for several benchmarks of heavy mediators. These are **A**:  $m_\phi = 1 \text{ MeV}$ ,  $g_e = 10^{-5}e$ ,  $\alpha_X = 0.1$ ; **B**:  $m_\phi = 10 \text{ MeV}$ ,  $g_e = 10^{-5}e$ ,  $\alpha_X = 0.1$ ; and **C**:  $m_\phi = 100 \text{ MeV}$ ,  $g_e = 10^{-4}e$ ,  $\alpha = 0.1$ . These depicted parameters obey all terrestrial and astrophysical constraints, though sub-MeV DM interacting with SM through a massive mediator may be strongly constrained by BBN; see text for details. The Xenon10 electron-ionization data bounds [34] are plotted in thin dashed gray. **In both panels**, the black solid (dashed) curve depicts the sensitivity reach of the proposed superconducting detectors, for a detector sensitivity to recoil energies between 1 meV–1 eV (10 meV–10 eV), with a kg-year of exposure. For comparison, the gray dot-dashed curve depicts the expected sensitivity utilizing electron ionization in a germanium target as obtained in Ref. [10].

kink in the colored curves as  $m_X$  increases arises when the stellar constraints evolve from cooling dominated by direct emission of  $\phi$  to the Higgstrahlung process (factoring in self-interaction constraints on  $\alpha_X$  at each  $m_X$ ). For mediator masses between an eV and  $\sim 10 \text{ keV}$ , direct detection cross sections are low on account of stellar emission constraints. These constraints are released as the mediators become more massive than the temperature of the star; supernova constraints instead become relevant, though trapping removes them for sufficiently large couplings.

Moving to heavy mediators, we focus on  $m_\phi \gtrsim \text{MeV}$ . A plethora of constraints exists in the literature for this mass range, see *e.g.* [29–32] in the context of kinetically mixed hidden photons. In the right panel of Fig. 2, we select several benchmark points, labeled **A–C**, that survive all terrestrial (*e.g.* beam dump) and stellar cooling constraints, and plot the resulting direct detection cross section of Eq. (3),  $\tilde{\sigma}_{\text{DD}}^{\text{heavy}}$ . Large couplings to electrons  $g_e \gtrsim 10^{-6}$  are possible despite stellar constraints due to trapping effects, and beam dump constraints may be evaded by decaying to additional particles in the dark sector. These statements hold regardless of the vector/scalar nature of the heavy mediator. However, for values of  $\alpha_X$  and  $g_e$  as large as these benchmark points, DM and/or the mediator will be brought into thermal equilibrium with the SM plasma. The chief constraint on these models is thus BBN and Planck limits on the number of relativistic species in equilibrium (see *e.g.* [33]).

The Planck constraints can be evaded; for instance coupling to  $\gamma/e$  through the time that the DM becomes non-relativistic will act to reduce the effective number of neutrinos at CMB epoch. On the other hand, during BBN, the helium fraction constrains the Hubble parameter, which is sensitive to all thermalized degrees of freedom. DM must then be either a real scalar or heavier than a few hundred keV in such simple models [33]. It follows that part of the depicted curves of benchmarks **A–C** in the low-mass region may not be viable; a detailed study of the viable parameter space is underway [18]. For completeness, we show the Xenon10 electron-ionization bounds [34] in the thin gray dashed curve. (The Xenon10 bounds on light mediators are not depicted in the left panel of Fig. 2 as they are orders of magnitude weaker than the parameter space shown.)

For comparison, we show the expected sensitivity using electron-ionization techniques with a germanium target as obtained in Ref. [10], translating their result into  $\tilde{\sigma}_{\text{DD}}$  of Eq. (3). These results are depicted by the dot-dashed gray curves in Fig. 2 for both the light (left panel) and heavy (right panel) mediator cases. For heavy mediators and  $m_X$  larger than a few hundred keV, our detection method is less sensitive than the projected one using germanium, while for lighter  $m_X$ , where electron ionization methods lose sensitivity, the superconducting devices win. (Indeed, this comparison between the detection methods is our main aim in presenting the right panel of Fig. 2.) In contrast, light mediators highlight the

strength of our proposed detectors. For DM masses above several hundred keV, superconducting detectors can outperform electron ionization techniques by several orders of magnitude. For dark matter below the MeV scale, the proposed superconducting detectors are uniquely staged to detect super light sub-MeV viable models of dark matter.

In summary, we have proposed a new class of detectors that utilize superconductors to detect electron recoils from thermal DM as light as a keV. Given some improvement over current technology, such detectors may have sufficiently low noise rates to be sensitive to the required energy scale of meV electron recoils. We have computed the DM scattering rates, taking into account Pauli blocking, and have shown that viable models may be detected. We hope this proof of concept encourages the experimental community to pursue research and development towards the feasibility of such devices, probing detection of DM down to the keV scale. We leave for future work the extended study of broader classes of DM models that may be detectable with these devices.

**Acknowledgments.** We thank Dave Moore, Joel Moore and Zohar Ringel for useful discussions, and Jeremy Mardon for helpful correspondence and comments on the manuscript. We are especially grateful to John Clarke and Matt Pyle for critical conversations on viable detector designs. The work of YH is supported by the U.S. National Science Foundation under Grant No. PHY-1002399. YH is an Awardee of the Weizmann Institute of Science – National Postdoctoral Award Program for Advancing Women in Science. YZ is supported by ERC Grant BSMOXFORD No. 228169. KZ is supported by the DoE under contract DE-AC02-05CH11231.

- 
- [1] E. Aprile *et al.* [XENON100 Collaboration], Phys. Rev. Lett. **109**, 181301 (2012) [arXiv:1207.5988 [astro-ph.CO]].
  - [2] D. S. Akerib *et al.* [LUX Collaboration], Phys. Rev. Lett. **112**, 091303 (2014) [arXiv:1310.8214 [astro-ph.CO]].
  - [3] R. Agnese *et al.* [SuperCDMS Collaboration], Phys. Rev. Lett. **112**, no. 24, 241302 (2014) [arXiv:1402.7137 [hep-ex]].
  - [4] D. E. Kaplan, M. A. Luty and K. M. Zurek, Phys. Rev. D **79**, 115016 (2009) [arXiv:0901.4117 [hep-ph]].
  - [5] K. M. Zurek, Phys. Rept. **537**, 91 (2014) [arXiv:1308.0338 [hep-ph]].
  - [6] Y. Hochberg, E. Kuflik, T. Volansky and J. G. Wacker, Phys. Rev. Lett. **113**, 171301 (2014) [arXiv:1402.5143 [hep-ph]].
  - [7] S. Tremaine and J. E. Gunn, Phys. Rev. Lett. **42**, 407 (1979).
  - [8] A. Boyarsky, O. Ruchayskiy and D. Iakubovskiy, JCAP **0903**, 005 (2009) [arXiv:0808.3902 [hep-ph]].
  - [9] A. Boyarsky, J. Lesgourgues, O. Ruchayskiy and M. Viel, JCAP **0905**, 012 (2009) [arXiv:0812.0010 [astro-ph]].
  - [10] R. Essig, J. Mardon and T. Volansky, Phys. Rev. D **85**, 076007 (2012) [arXiv:1108.5383 [hep-ph]].
  - [11] P. W. Graham, D. E. Kaplan, S. Rajendran and M. T. Walters, Phys. Dark Univ. **1**, 32 (2012) [arXiv:1203.2531 [hep-ph]].
  - [12] A. J. Miller, S. W. Nam, J. M. Martinis and A. V. Sergienko, Appl. Phys. Lett. **83**, 791 (2003).
  - [13] D. J. Goldie, A. V. Velichko, D. M. Glowacka and S. Withington, J. Appl. Phys. **109**, 084507 (2011).
  - [14] B. S. Karasik, S. V. Pereverzev, A. Soibel, D. F. Santavica, D. E. Prober, D. Olaya and M. E. Gershenson Appl. Phys. Lett. **101**, 052601 (2012).
  - [15] S. Reddy, M. Prakash and J. M. Lattimer, Phys. Rev. D **58**, 013009 (1998) [astro-ph/9710115].
  - [16] J. N. Bahcall and R. K. Ulrich, Rev. Mod. Phys. **60**, 297 (1988).
  - [17] J. N. Bahcall, Phys. Rev. C **56**, 3391 (1997) [hep-ph/9710491, hep-ph/9710491].
  - [18] Y. Hochberg, Y. Zhao and K. M. Zurek, work in progress.
  - [19] G. J. Feldman and R. D. Cousins, Phys. Rev. D **57**, 3873 (1998), physics/9711021.
  - [20] H. An, M. Pospelov and J. Pradler, Phys. Lett. B **725**, 190 (2013) [arXiv:1302.3884 [hep-ph]].
  - [21] H. An, M. Pospelov and J. Pradler, Phys. Rev. Lett. **111**, 041302 (2013) [arXiv:1304.3461 [hep-ph]].
  - [22] D. Clowe, A. Gonzalez and M. Markevitch, Astrophys. J. **604**, 596 (2004) [astro-ph/0312273].
  - [23] M. Markevitch, A. H. Gonzalez, D. Clowe, A. Vikhlinin, L. David, W. Forman, C. Jones and S. Murray *et al.*, Astrophys. J. **606**, 819 (2004) [astro-ph/0309303].
  - [24] S. W. Randall, M. Markevitch, D. Clowe, A. H. Gonzalez and M. Bradac, Astrophys. J. **679**, 1173 (2008) [arXiv:0704.0261 [astro-ph]].
  - [25] M. Rocha, A. H. G. Peter, J. S. Bullock, M. Kaplinghat, S. Garrison-Kimmel, J. Onorbe and L. A. Moustakas, Mon. Not. Roy. Astron. Soc. **430**, 81 (2013) [arXiv:1208.3025 [astro-ph.CO]].
  - [26] A. H. G. Peter, M. Rocha, J. S. Bullock and M. Kaplinghat, arXiv:1208.3026 [astro-ph.CO].
  - [27] S. Tulin, H. B. Yu and K. M. Zurek, Phys. Rev. Lett. **110**, no. 11, 111301 (2013) [arXiv:1210.0900 [hep-ph]].
  - [28] S. D. McDermott, H. B. Yu and K. M. Zurek, Phys. Rev. D **83**, 063509 (2011) [arXiv:1011.2907 [hep-ph]].
  - [29] J. D. Bjorken, R. Essig, P. Schuster and N. Toro, Phys. Rev. D **80**, 075018 (2009) [arXiv:0906.0580 [hep-ph]].
  - [30] H. K. Dreiner, J. F. Fortin, C. Hanhart and L. Ubaldi, Phys. Rev. D **89**, no. 10, 105015 (2014) [arXiv:1310.3826 [hep-ph]].
  - [31] H. K. Dreiner, J. F. Fortin, J. Isern and L. Ubaldi, Phys. Rev. D **88**, 043517 (2013) [arXiv:1303.7232 [hep-ph]].
  - [32] B. Batell, R. Essig and Z. Surujon, Phys. Rev. Lett. **113**, no. 17, 171802 (2014) [arXiv:1406.2698 [hep-ph]].
  - [33] Cl. Boehm, M. J. Dolan and C. McCabe, JCAP **1308**, 041 (2013) [arXiv:1303.6270 [hep-ph]].
  - [34] R. Essig, A. Manalaysay, J. Mardon, P. Sorensen and T. Volansky, Phys. Rev. Lett. **109**, 021301 (2012) [arXiv:1206.2644 [astro-ph.CO]].